NASA/TM—2013-217837

# Wind-US Code Contributions to the First AIAA Shock Boundary Layer Interaction Prediction Workshop

*Nicholas J. Georgiadis, Manan A. Vyas, and Dennis A. Yoder*
*Glenn Research Center, Cleveland, Ohio*

February 2013

# NASA STI Program . . . in Profile

Since its founding, NASA has been dedicated to the advancement of aeronautics and space science. The NASA Scientific and Technical Information (STI) program plays a key part in helping NASA maintain this important role.

The NASA STI Program operates under the auspices of the Agency Chief Information Officer. It collects, organizes, provides for archiving, and disseminates NASA's STI. The NASA STI program provides access to the NASA Aeronautics and Space Database and its public interface, the NASA Technical Reports Server, thus providing one of the largest collections of aeronautical and space science STI in the world. Results are published in both non-NASA channels and by NASA in the NASA STI Report Series, which includes the following report types:

- TECHNICAL PUBLICATION. Reports of completed research or a major significant phase of research that present the results of NASA programs and include extensive data or theoretical analysis. Includes compilations of significant scientific and technical data and information deemed to be of continuing reference value. NASA counterpart of peer-reviewed formal professional papers but has less stringent limitations on manuscript length and extent of graphic presentations.

- TECHNICAL MEMORANDUM. Scientific and technical findings that are preliminary or of specialized interest, e.g., quick release reports, working papers, and bibliographies that contain minimal annotation. Does not contain extensive analysis.

- CONTRACTOR REPORT. Scientific and technical findings by NASA-sponsored contractors and grantees.

- CONFERENCE PUBLICATION. Collected papers from scientific and technical conferences, symposia, seminars, or other meetings sponsored or cosponsored by NASA.

- SPECIAL PUBLICATION. Scientific, technical, or historical information from NASA programs, projects, and missions, often concerned with subjects having substantial public interest.

- TECHNICAL TRANSLATION. English-language translations of foreign scientific and technical material pertinent to NASA's mission.

Specialized services also include creating custom thesauri, building customized databases, organizing and publishing research results.

For more information about the NASA STI program, see the following:

- Access the NASA STI program home page at *http://www.sti.nasa.gov*

- E-mail your question to *help@sti.nasa.gov*

- Fax your question to the NASA STI Information Desk at 443–757–5803

- Phone the NASA STI Information Desk at 443–757–5802

- Write to:
  STI Information Desk
  NASA Center for AeroSpace Information
  7115 Standard Drive
  Hanover, MD 21076–1320

NASA/TM—2013-217837

# Wind-US Code Contributions to the First AIAA Shock Boundary Layer Interaction Prediction Workshop

*Nicholas J. Georgiadis, Manan A. Vyas, and Dennis A. Yoder*
*Glenn Research Center, Cleveland, Ohio*

National Aeronautics and
Space Administration

Glenn Research Center
Cleveland, Ohio 44135

February 2013

## Acknowledgments

This work was jointly sponsored by the Department of Defense (DoD) Test Resource Management Centers (TRMC) Test and Evaluation/Science and Technology (T&E/S&T) Program through the High Speed Systems Test (HSST) area (formerly APTT) and the NASA Fundamental Aeronautics Hypersonics Project.

This work was sponsored by the Fundamental Aeronautics Program
at the NASA Glenn Research Center.

*Level of Review*: This material has been technically reviewed by technical management.

Available from

NASA Center for Aerospace Information
7115 Standard Drive
Hanover, MD 21076–1320

National Technical Information Service
5301 Shawnee Road
Alexandria, VA 22312

Available electronically at http://www.sti.nasa.gov

# Wind-US Code Contributions to the First AIAA Shock Boundary Layer Interaction Prediction Workshop

Nicholas J. Georgiadis, Manan A. Vyas, and Dennis A. Yoder
National Aeronautics and Space Administration
Glenn Research Center
Cleveland, Ohio 44135

## Abstract

**This report discusses the computations of a set of shock wave / turbulent boundary layer interaction (SWTBLI) test cases using the Wind-US code, as part of the 2010 American Institute of Aeronautics and Astronautics (AIAA) shock / boundary layer interaction workshop. The experiments involve supersonic flows in wind tunnels with a shock generator that directs an oblique shock wave toward the boundary layer along one of the walls of the wind tunnel. The Wind-US calculations utilized structured grid computations performed in Reynolds-averaged Navier-Stokes mode. Four turbulence models were investigated: the Spalart-Allmaras one-equation model, the Menter Baseline and Shear Stress Transport k-$\omega$ two-equation models, and an explicit algebraic stress k-$\omega$ formulation. Effects of grid resolution and upwinding scheme were also considered. The results from the CFD calculations are compared to particle image velocimetry (PIV) data from the experiments. As expected, turbulence model effects dominated the accuracy of the solutions with upwinding scheme selection indicating minimal effects.**

## Nomenclature

| | |
|---|---|
| $k$ | turbulent kinetic energy |
| $M_\infty$ | freestream Mach number |
| $u$ | axial velocity |
| $v$ | normal velocity |
| $x, y, z$ | Cartesian coordinates |
| $y^+$ | wall normal coordinate |
| $\delta$ | boundary layer thickness |
| $\epsilon$ | turbulent dissipation rate |
| $\mu$ | dynamic molecular viscosity |
| $\mu_t$ | dynamic eddy viscosity |
| $\omega$ | specific turbulent dissipation rate $= \epsilon/k$ |
| $\theta$ | shock generator angle |

## Introduction

In supersonic flows, the shock wave / turbulent boundary layer interaction (SWTBLI) is a very common phenomena that has significant effects on the operability of specific components such as aircraft inlets and also on overall performance of aerospace vehicles. The problem has been studied extensively over the past few decades in laboratory experiments and in computational fluid dynamics (CFD) efforts. While gains in understanding of the underlying fluid dynamics of SWTBLI have been made, research continues into understanding the complex interaction of a shock wave with a turbulent boundary layer. In a typical SWTBLI, the adverse pressure gradient induced by the shock system causes a flow separation that frequently

is unsteady and three-dimensional. Without question, control of SWTBLI has yet to be mastered. While there have been numerous CFD studies, there is not a single approach that has been identified as optimal for calculation of SWTBLI.

Until recently, Reynolds-averaged Navier-Stokes (RANS) methods were used almost exclusively, and for practical aerodynamic analyses that contain one or more SWTBLIs, RANS is still the only feasible approach. More recently, large eddy simulation (LES) and hybrid RANS-LES techniques have been investigated for application to the SWTBLI problem, but typically have been restricted to small subset problems, as applying an LES-based technique to a more complex system (i.e. aircraft inlet) involving SWTBLIs is still largely prohibitive due to the large range of scales that are important. Knight and Degrez[1] and Knight et al[2] provide comprehensive overviews of a broad range in CFD methods as applied to SWTBLIs, in particular those investigated under AGARD and RTO working groups. Consideration of both RANS and LES methods is made. Reference 3 focuses on an assessment of RANS-based methods while a survey of LES-based approaches as applied to SWTBLIs is presented in Edwards.[4] The overall conclusions of these survey papers is that RANS methods are inherently unable to calculate some of the crucial features of SWTBLI, in particular the unsteadiness of the shock system and separated flow. In addition, the three dimensional features are also troublesome for RANS-based techniques. LES-based techniques may be promising, but neither sufficient maturity of these techniques nor understanding of their ability to properly handle the underlying fluid dynamics has been realized.

A recent workshop considering CFD calculations for a set of SWTBLI cases was held in conjunction with the 48th American Institute of Aeronautics and Astronautics (AIAA) Aerospace Sciences Meeting. An overview of the workshop objectives is presented in Benek[5] with a summary of overall findings presented in Benek and Babinsky.[6] The focus of this workshop was SWTBLI as occurs in supersonic inlets. Several investigators contributed solutions to this workshop. Contributions included RANS and LES-based computations. DeBonis et al[7] provides a comprehensive assessment of the CFD calculations, including uncertainty analysis of the submitted CFD results and experimental data obtained for the same configurations. Hirsch[8] examined some of the CFD trends, in particular effects of turbulence modeling, RANS versus LES, and numerical schemes submitted by several investigators and includes the results from our efforts described herein.

In this paper, we discuss the solutions obtained with the Wind-US code for the two sets of cases that were the focus of the SWTBLI workshop. A brief description of the test cases is provided first. The CFD approach is presented next including construction of the computational grids, turbulence models used, and other code settings. Comparisons of CFD calculations to experimental data for the test cases are presented, followed by conclusions.

## Experimental Configurations

The experimental data set for the first SWTBLI test case was obtained at the Institut Universitaire des Systemes Thermiques Industriels (IUSTI) in Marseille, France.[9] The experimental data was utilized in the European Union SWTBLI research project referred to as UFAST.[10] The UFAST experiments utilized an 8 degree shock generator which spanned the entire width of the tunnel with an approaching Mach 2.25 flow. The supply stagnation pressure was 50.5 kPa and the stagnation temperature was 293 K.

The second SWTBLI test case was investigated at the University of Michigan (UM)[11] as part of the Collaborative Center for the Aeronautical Sciences (CCAS) sponsored by the United States Air Force. The UM experiments utilized three shock generator angles with an approaching Mach 2.75 flow. The shock angles were 7.75, 10.0 and 12.0. The supply stagnation pressure was 101.0 kPa and the stagnation temperature was 293 K. Unlike the UFAST experiments, the UM shock generators did not span the entire width of the wind tunnel and were supported by a strut from the top of the wind tunnel.

A schematic of the experimental configuration generally representing that used in both sets of experiments is shown in Fig. 1 as taken from DeBonis et al.[7] Cross sectional views of these two cases are provided in Fig. 2. Particle Image Velocimetry (PIV) was used in all cases to characterize the interaction regions, with both mean flow velocities and turbulent statistics obtained. Specifics of the experimental measurements are discussed in Ref. 10 for the UFAST case and in Ref. 11 for the UM case.

## CFD Approach

The CFD calculations described in this report used the Wind-US code, which is the production RANS solver of the NPARC Alliance, a formal partnership of NASA Glenn Research Center (GRC) and the U.S. Air Force Arnold Engineering Development Center (AEDC), with significant participation by the Boeing Company. An overview of the current capabilities in the Wind-US flow solver may be found in Nelson[12] and Georgiadis et al.[13] This section describes the computational grids generated for these SWTBLI cases, numerical schemes examined, and turbulence models utilized as part of this study.

### Computational Grids

The Wind-US calculations described in this report utilized structured grid computations performed in RANS mode. Rumsey presented results obtained with the CFL3D CFD code in Ref. 14, obtained using the same computational grids that were constructed for simulations described in this report. The UFAST grid is shown in Fig. 3. The overall grid had approximately 7.4 million points spread across 10 structured grid zones. Point-to-point connectivity was used at zonal interfaces through most of the overall grid, with mismatched zones just upstream and downstream of the interaction region, shown in Fig. 3(b), in order to allow greater resolution in the SWTBLI focused region. Walls were packed such that the first point was placed at a position corresponding to a nominal y+ of approximately 1.0, using the fully expanded tunnel conditions corresponding to Mach 2.25 flow and an assumed reference skin friction coefficient of 0.0025. One half of the geometry was modeled with a symmetry plane placed at the middle of the spanwise direction.

The computational grid for the UM case (7.75 degree shock generator) is shown in Fig. 4. The grids for the 10 degree and 12 degree shock generator were built in exactly the same manner as was the 7.75 degree case. Each grid had approximately 8.4 million points spread across 16 structured grid zones. The same grid strategy was utilized as for the UFAST case, i.e. walls were packed to a nominal y+ =1.0 and point-to-point connectivity was used everywhere except just upstream and downstream of the interaction regions. As discussed in the experimental configurations section, the UM shock generator did not span the entire width of the tunnel, and was mounted via a support strut originating in the tunnel ceiling. All of these details were modeled in the computational grids constructed here. One half of the geometry was modeled with the symmetry plane placed at the middle of the spanwise direction and cutting through the center of the support strut.

### Numerical Schemes

Three spatial flux methods available in Wind-US were investigated for the UM test case. The first is the Roe scheme,[15] which is the default setting in Wind-US. The second is the well known method due to Van Leer,[16] and the third is that of Harten et al[17] as modified by Toro[18] and commonly referred to as the HLLC scheme. Second order schemes were used in all cases with TVD limiters applied. For the UFAST case, only the default 2nd order Roe scheme was utilized.

### Turbulence Modeling

As discussed in the introduction, turbulence modeling has been found to be the most important factor affecting the calculation of SWTBLI, and was the focus of efforts described in this report. In Wind-US and many production CFD solvers, the Shear-Stress Transport (SST) two-equation turbulence model of Menter[19] is widely used because it is robust and accurate for a broad range of flows, including wall boundary layers and free shear layer regions. The SST model is a two-layer model which employs the $k-\omega$ model of Wilcox[20] in the inner region of boundary layers and switches to a $k-\epsilon$ model in the outer region of boundary layers and in mixing regions. The outer $k-\epsilon$ model is transformed to provide a second set of $k-\omega$ equations with a blending function used to transition between the two sets of equations. A modification to the eddy viscosity limits the shear stress, per the Bradshaw assumption that the shear stress in a boundary layer is proportional to the turbulent kinetic energy. The SST model has been found to provide reasonably accurate calculations of wall bounded flows, provided there are not large flow separations. The second turbulence model used here was the Menter baseline (BSL) $k-\omega$ model, which is the very close relative of the Menter SST formulation. It is also a two layer model, with primary difference being the absence of the shear stress limiter that is employed with SST.

The third turbulence model investigated in this study is the one-equation model due to Spalart and Allmaras.[21,22] We will refer to this model in this report as the "SA" model.

The fourth turbulence model investigated in these SWTBLI cases is a $k-\omega$ based non-linear explicit algebraic stress model (ASM) formulation based on the work of Rumsey.[23] Unlike linear two-equation models, ASM formulations are sensitive to turbulent stress anisotropies and have a direct relation to the full Reynolds stress model. As a result, ASMs have the capability to include more relevant flow physics than the linear models. However, they are also solved using a two-equation approach and as a result are not significantly more computationally expensive than linear two-equation models. In Ref. 13, Wind-US was applied to a Mach 5 SWTBLI problem using the SST and k-$\omega$ models. These models provided similar predictions of skin friction coefficient for this test case. A linear k-$\epsilon$ model and k-$\epsilon$ based ASM were also applied to this problem and significantly overpredicted the skin friction coefficient downstream of the key interaction region. Because of this result and similar findings by other investigators employing k-$\epsilon$ models for SWTBLI problems, we did not examine k-$\epsilon$ models in this work.

## UFAST Test Case

The Mach number approaching the SWTBLI region for the UFAST case is lower than that for the UM case and as a result, the oblique shock wave angle is higher than for the UM test case. In turn, the resultant adverse pressure gradient effects are actually relatively stronger through the SWTBLI region. Axial velocity contours for the UFAST test case obtained with the SST turbulence model are shown in Fig. 5. The oblique wave originating from the sharp leading edge of the shock generator may be observed, along with the SWTBLI region centered about $x = 320mm$. The complex interaction on the top of the tunnel results in a flow separation that is much larger than that in the SWTBLI focus region and resulted in unsteadiness that was sustained even after the focus SWTBLI region on the bottom stopped changing and was considered to be converged. Eddy viscosity contours corresponding to the flowfield solution shown in Fig. 5 are shown in Fig. 6. The eddy viscosity values shown are normalized by the local molecular viscosity. For plotting purposes, the normalized eddy viscosity values shown are capped at $\mu_t/\mu = 500$ for clarity in the focus region although the maximum values in the region near the top of the domain reached nearly 1500.

The experimental data was collected within a select region around the bottom wall interaction. Axial velocity contours for the UFAST test case using the four turbulence modeling approaches are compared to the experimental PIV measurements in Fig. 7. As will be the case for the UM experiments discussed in the next section, the CFD solution slices represent the same physical domain, with the same contour levels as the experimental data. Further, the CFD solutions were interpolated to the same physical locations where the PIV data were taken, as was required by the organizers of the AIAA workshop, for purposes of computing differences between solutions and experimental data.[7] Examining these contours, the extent of the adverse pressure gradient effects indicated by the Menter SST solution are larger than the other solutions and experimental data.

Further comparisons of the CFD solutions and experimental data are made for the axial velocity profiles at four axial locations in Fig. 8. One may observe that the CFD solutions plotted do not go all the way to the wall, and again this is due to interpolation of the CFD results to the PIV measurement locations. While most CFD-to-experimental comparisons are made with the CFD solutions actually plotted at the computational grid points, the manner of comparison used here and in the workshop does allow one to determine what the CFD would predict with a "probe" placed at a specific location, in analogy to the experiments. For this case and the UM cases, however, with a rather fine experimental PIV grid, there are no observable differences between plotted lines using the CFD solutions mapped to the experimental physical locations and the CFD solutions at the actual computational grid points.

The comparisons in Fig. 8 show the same trends as indicated by the contour plots of Fig. 7. In particular, the size of the flow separation indicated by the SST solution is greater than that indicated by the experimental data and the other turbulence models. One may note an especially large difference between the Menter SST and BSL results, which is due to the eddy viscosity limiter in the SST formulation. Normal velocity profiles are compared in Fig. 9. While the most commonly used quantity for comparing boundary layer profiles is axial velocity, these normal velocity comparisons show how substantial the effect of turbulence model is on the boundary layer details, and in particular how none of the models are able to capture the behavior indicated by the experimental data.

## University of Michigan (UM) Test Case

As described previously, three shock generator configurations were examined as part of the UM experiments. For the first case with shock generator angle set to 7.75 degrees, experimental data was made available to CFD analysts prior to the workshop, and is the focus of the discussion in this section. Data for the other two test cases was held back to enable "blind" comparisons of experimental data and submitted CFD solutions. From our calculations with Wind-US using the SST turbulence model, axial velocity contours for all three UM test cases, where the shock generator angle was varied, are shown in Fig. 10. Eddy viscosity contours for the UM test case are shown in Fig. 11. As expected, the strength and size of the interaction increases with larger shock generator angle. The focus of the comparisons between solutions at the workshop was made for the smallest shock generator angle, 7.75 degrees, and we will concentrate on this case for the remainder of this discussion. For simplicity, we will refer to this as the "UM test case."

Axial velocity contours for the UM test case in the SWTBLI focus region using the four turbulence modeling approaches are compared to experimental measurements in Fig. 12. As discussed for the UFAST test case, the CFD solution slices represent the same physical domain, with the same contour levels as the experimental data, and with the CFD solutions interpolated to the experimental measurement locations. Normal velocity contours are compared in Fig. 13 and contours of the velocity shear component are shown in Fig. 14.

Further comparisons of the CFD solutions and experimental data are made for the axial velocity profiles at four axial locations in Fig. 15. In this and subsequent figures, two sets of experimental data are also presented. The first was obtained with stereoscopic PIV measured along spanwise (or "yz cut") planes at seven axial locations, and the second along a streamwise plane, referred to in the figures as "xy cut." In the UFAST experiments, the lower approaching Mach number (2.25 in UFAST versus 2.75 in UM) produces a steeper shock wave (approximately 33 degrees versus 27 degrees) for a very similar wedge angle (8.0 degrees versus 7.75 degree). This results in a relatively stronger interaction region, and flow separation, while such a flow separation is not obvious for this lowest wedge angle case in the UM experiments.

All of the turbulence modeling approaches show a smaller effect of the shock interaction on the boundary layer thickening than indicated by the experiment with the SST solution being closest to the data. Recall that back in the UFAST results with flow separation, the SA and ASM results indicated smaller effects of shock interaction on boundary layer thickening, with SST indicating too large of a response relative to the experimental data. These results are very similar to those reported for SA and SST by Bhagwandin and DeSpirito[24] and also to other participants in the workshop as shown in Ref. 8. Normal velocity profiles are compared in Fig. 16 and show considerable scatter among the turbulence models and magnify the discrepancies with experimental data in the SWTBLI region.

Using the grid sequencing capability within Wind-US, a grid sensitivity study was made for SST turbulence model solutions using the complete grid and the sequenced grid where every other point in each computational direction, termed "medium" was used. Recalling that the full (fine) grid had 8.4 million points, the medium grid had approximately 1 million total points. A comparison of axial and normal velocities using the two grid levels is provided in Fig. 17. This does not suffice as a thorough grid sensitivity study as a grid independent solution was not achieved. While the qualitative behavior is similar between the fine and medium grids, especially in the axial velocity profiles, it appears that the near wall behavior is less affected by removing every other grid point as is the behavior near the top of the boundary layer. This is not surprising, as with the wall spacing set to a nominal y+ of 1, removing every other grid point still has the first point well within the laminar sublayer. It does emphasize the need to consider grid resolution away from the wall, however, for cases that are not straightforward equilibrium boundary layers.

An investigation of the effects of upwinding scheme, also using the Menter SST model, is provided in Fig. 18. In all cases, second order versions of the Roe, Van Leer, and HLLC schemes were used and there appears to be minimal effect of the upwinding scheme on prediction of the SWTBLI region. Interestingly, Rumsey found more significant effects of upwinding scheme when using the SA turbulence model on the same computational grids as we have employed here. Our finding, from consideration of the differences observed among turbulence models and upwinding schemes, is that turbulence model effects dominate the accuracy of SWTBLI calculations.

## Conclusions

Two sets of SWTBLI flows were investigated using the Wind-US CFD code, in efforts towards participating in the 2010 AIAA Shock Boundary Layer Interaction Prediction Workshop. The results obtained here were qualitatively similar to most of the results obtained by investigators of other similar RANS flow solvers, indicating that the capabilities of most mature production flow CFD solvers are comparable, especially when using similar turbulence modeling and numerical schemes. Further, it appears that turbulence modeling remains the pacing technology affecting the accuracy of SWTBLI simulations.

Calculations used the SA one-equation turbulence model and SST two-equation turbulence model, which were not only used by other participants in this workshop for their simulations of the same SWTBLI cases, but are two of the most widely used RANS models in the aerospace community for calculating boundary layer dominated flow problems in RANS mode. While the qualitative agreement with experimental data may be considered acceptable, the boundary layer details were not accurate. We also obtained calculations using the Menter BSL two-equation model and an explicit algebraic stress model which did not provide better results than the linear turbulence models. Comparison of the BSL and SST results illustrated effects of the shear stress limiter. For SWTBLI flows without separation, the SST performs well as shown by the UM results. Once separation occurs, however, the SST model tends to over-react relative to BSL, as was shown by the UFAST results. At the workshop, some attempts at using LES based techniques were presented, but production usage of LES for complex SWTBLI dominated flows is far from a mature science. A few key limitations are difficulties in prescribing sufficient inflow turbulent boundary conditions, simulating experiments at the actual Reynolds numbers investigated, and when employing hybrid RANS-LES approaches, the manner in which the switch from a RANS region to an LES region is handled. As computer resources, including processor speed, available memory, and storage capacity improve, LES-based methods will become more practical.

In the near term, there still is a need for RANS model improvements, and RANS will still likely be the technique of choice for some time in concept screening and evaluation. There has been little effort in the past decade to improve pure RANS models. Most interest and support in the area of turbulent flow computations has been in the area of LES and hybrids. Some investment in RANS-based methods still seems warranted.

## References


[1]Knight, D. and Degrez, G., "Shock Wave / Boundary Layer Interactions in High Mach Number Flows - A Critical Survey of Current CFD Prediction Capability," *AGARD AR-319*, Vol. 2, 1998.

[2]Knight, D., Yan, H., Panaras, A. G., and Zheltovodov, A., "Advances in CFD Prediction of Shock Wave Turbulent Boundary Layer Interactions," *Progress in Aerospace Sciences*, Vol. 39, No. 2, February 2003, pp. 121–184.

[3]Zheltovodov, A. A., "Some Advances in Research of Shock Wave Turbulent Boundary Layer Interactions," AIAA Paper 2006-0496, January 2006.

[4]Edwards, J. R., "Numerical Simulations of Shock/Boundary Layer Interactions Using Time-Dependent Modeling Techniques: A Survey of Recent Results," *Progress in Aerospace Sciences*, Vol. 44, No. 6, Aug. 2008, pp. 447–465.

[5]Benek, J., "Overview of the 2010 AIAA Shock Boundary Layer Interaction Workshop," AIAA Paper 2010-4821, January 2010.

[6]Benek, J. and Babinsky, H., "Lessons Learned from the 2010 AIAA Shock Boundary Layer Interaction Workshop," AIAA Paper 2010-4825, January 2010.

[7]DeBonis, J. R., Oberkampf, W. L., Wolf, R. T., Orkwis, P. D., Turner, M. G., Babinsky, H., and Benek, J. A., "Assessment of Computational Fluid Dynamics and Experimental Data for Shock Boundary-Layer Interactions," *AIAA Journal*, Vol. 50, No. 4, Apr. 2012, pp. 891–903.

[8]Hirsch, C., "SBLI Lessons Learned - CFD Simulations of Two Test Cases ," AIAA Paper 2010-4824, January 2010.

[9]Dupont, P., Piponniau, S., Sidorenko, A., and Debieve, J., "Investigation by Particle Image Velocimetry Measurements of Oblique Shock Reflection with Separation," *AIAA Journal*, Vol. 46, No. 6, 2008, pp. 1365–1370.

[10]*Unsteady Effects in Shock Wave Induced Separation*, edited by P. Doerffer, C. Hirsch, J.-P. Dussauge, H. Babinsky, and G. Barakos, Springer, 2010.

[11]Lapsa, A. P. and Dahm, W. J. A., "Stereo Particle Image Velocimetry of Nonequilibrium Turbulence Relaxation in a Supersonic Boundary Layer," *Experiments in Fluids*, Vol. 50, No. 1, 2011, pp. 89–108.

[12]Nelson, C., "An Overview of the NPARC Alliance's Wind-US Flow Solver," AIAA Paper 2010-27, January 2010.

[13]Georgiadis, N. J., Yoder, D. A., Towne, C. E., Engblom, W. A., Bhagwandin, V., Power, G. D., Lankford, D. W., and Nelson, C. C., "Wind-US Physical Modeling Improvements to Complement Hypersonic Testing and Evaluation," AIAA Paper 2009-193, January 2009.

[14]Rumsey, C. L., "CFL3D Contribution to the AIAA Supersonic Shock Boundary Layer Interaction Workshop," NASA TM 2010-216858, October 2010.
[15]Roe, P. L., "Approximate Riemann Solvers, Parameter Vectors, and Difference Schemes," *J. Comp. Phys.*, Vol. 43, 1981, pp. 357–372.
[16]van Leer, B., "Towards the Ultimate Conservative Difference Schemes V. A Second Order Sequel to Godunov's Method," *J. Comp. Phys.*, Vol. 32, 1979, pp. 101–136.
[17]Harten, A., Lax, P., and Leer, B. V., "On upstream differencing and Godunov-type schemes for hyperbolic conservation laws," *SIAM Rev.*, Vol. 25, 1982, pp. 35–61.
[18]Toro, E. F., Spruce, M., and Speares, W., "Restoration of the contact surface in the HLL-Riemann solver," *Shock Wave*, Vol. 4, 1994, pp. 25–34.
[19]Menter, F. R., "Zonal Two Equation $k-\omega$ Turbulence Models for Aerodynamic Flows," *AIAA Journal*, Vol. 32, No. 8, 1994, pp. 1598–1605.
[20]Wilcox, D. C., "Reassessment of the Scale-Determining Equation for Advanced Turbulence Models," *AIAA Journal*, Vol. 26, No. 11, February 1988, pp. 1299–1310.
[21]Spalart, P. R. and Allmaras, S. R., "A One-Equation Turbulence Model for Aerodynamic Flows," AIAA Paper 92-0439, 1992.
[22]Spalart, P. R. and Allmaras, S. R., "A One-Equation Turbulence Model for Aerodynamic Flows," *La Recherche Aerospatiale*, No. 1, 1994, pp. 5–21.
[23]Rumsey, C. L., Gatski, T. B., and Morrison, J. H., "Turbulence Model Predictions of Strongly Curved Flow in a U-Duct," *AIAA Journal*, Vol. 38, No. 8, August 2000, pp. 1394–1402.
[24]Bhagwandin, V. A. and DeSpirito, J., "Numerical Prediction of Supersonic Shock Boundary-Layer Interaction," AIAA Paper 2011-859, January 2011.

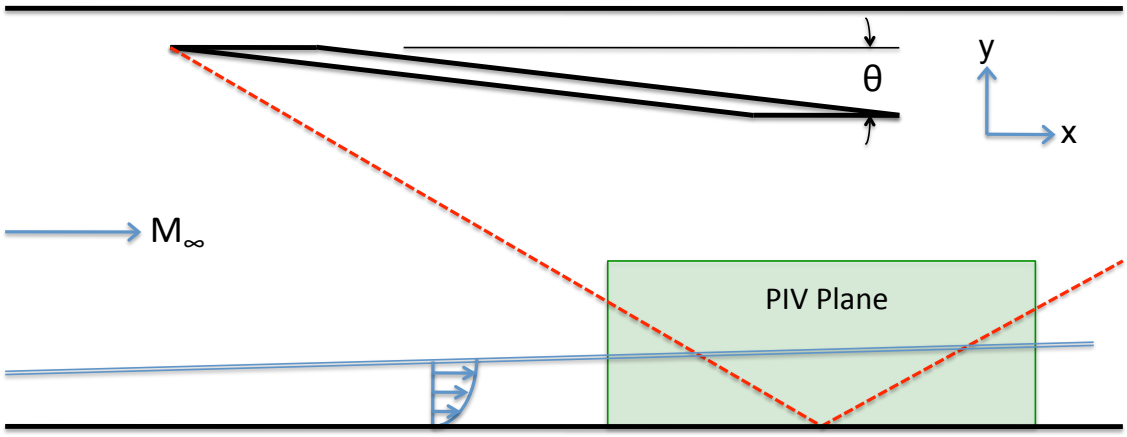


**Figure 1. Schematic of SWTBLI experimental configuration (courtesy of DeBonis et al[7]).**

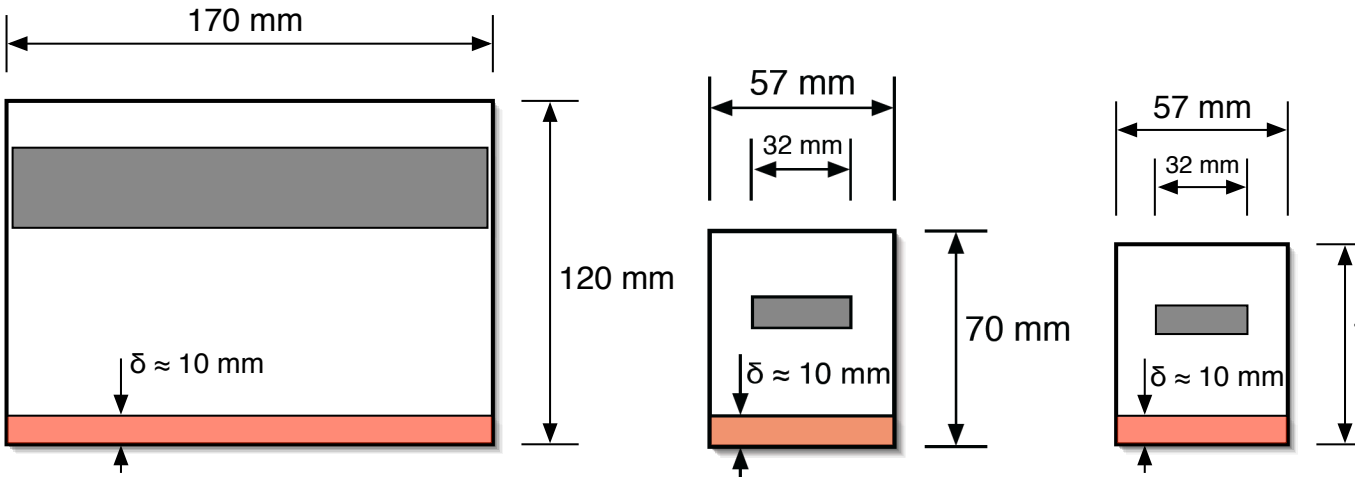


(a) UFAST (b) UM

**Figure 2. Cross sectional views of SWTBLI test configurations (courtesy of DeBonis et al[7]).**

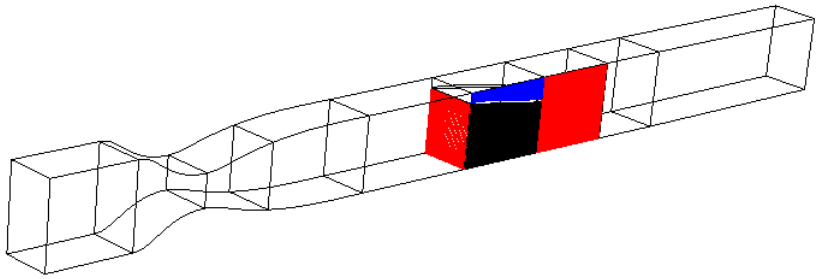

(a) entire domain

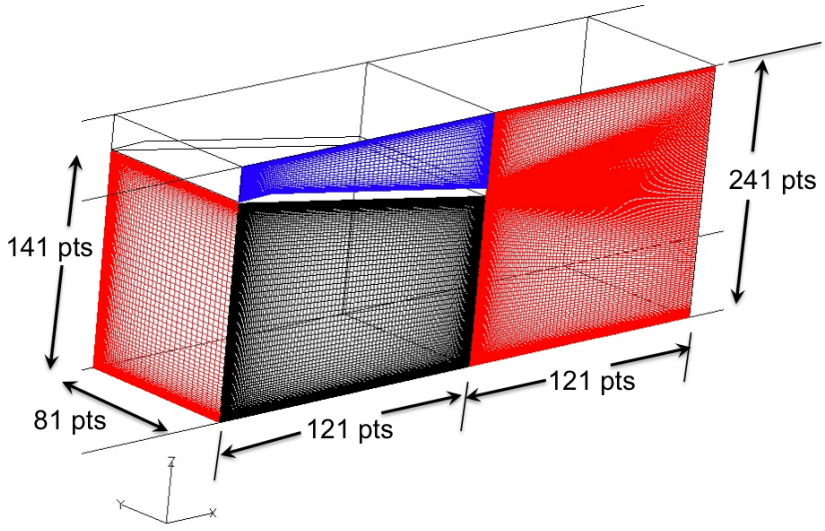


(b) detail near shock generator

**Figure 3. Computational grid for UFAST test case.**

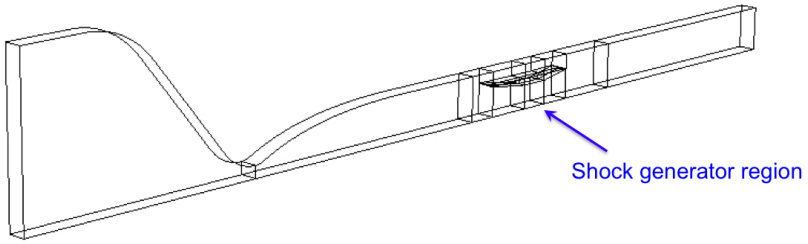


(a) entire domain

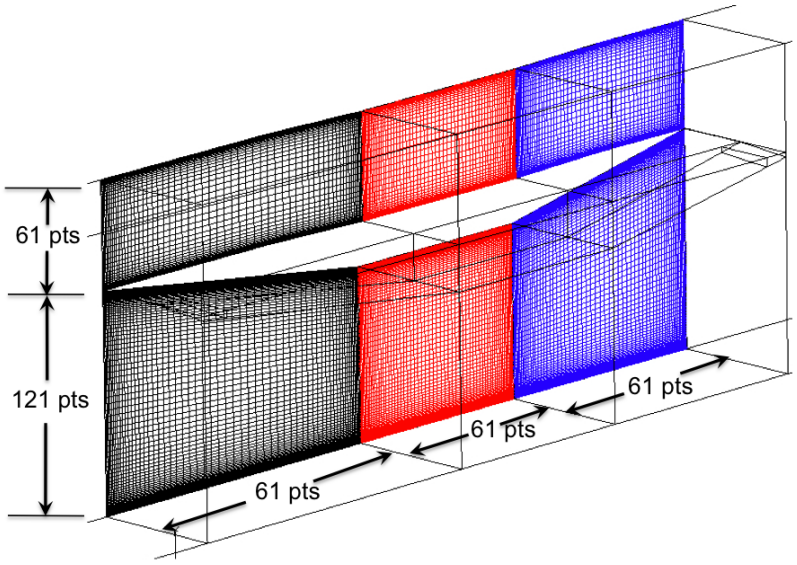


(b) streamwise detail near shock generator

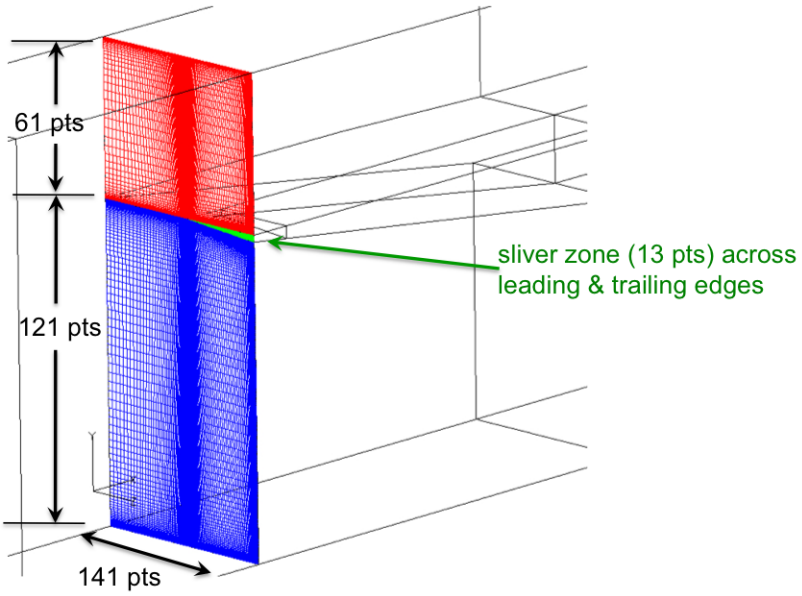


(c) spanwise detail near shock generator

**Figure 4. Computational grid for UM test case.**

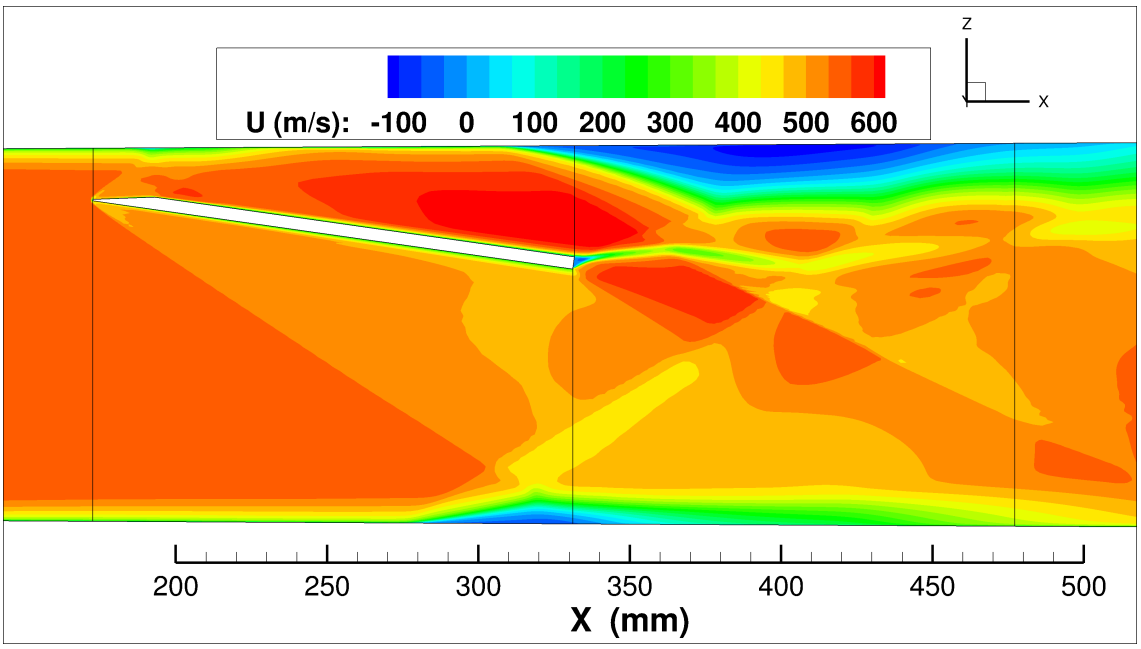


**Figure 5. Velocity contours for UFAST test case using SST.**

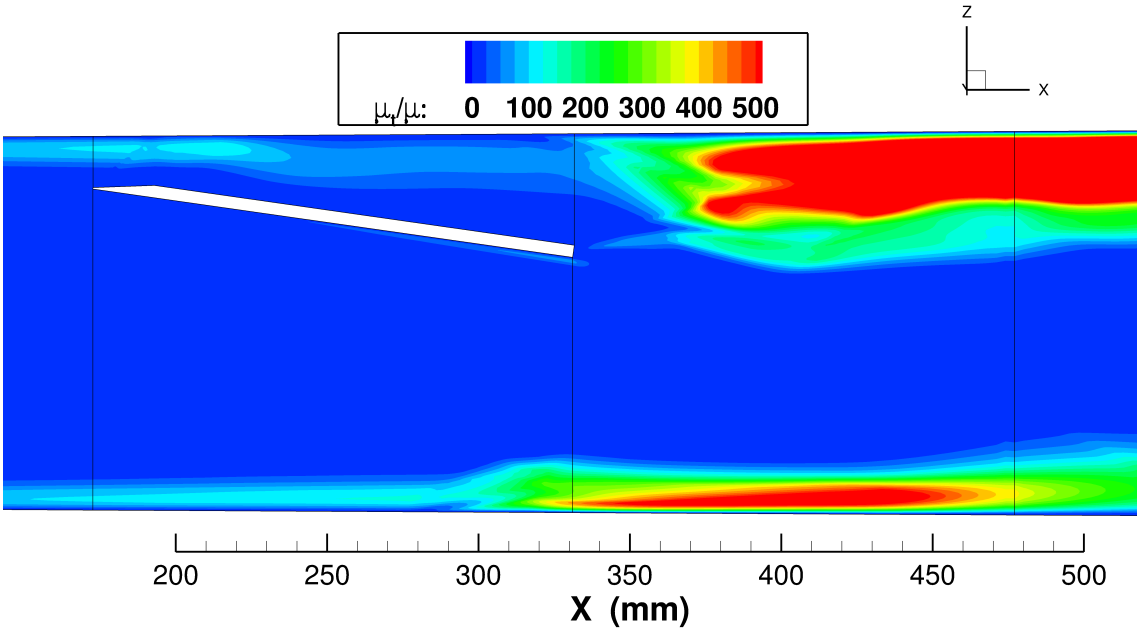


**Figure 6. Normalized eddy viscosity contours for UFAST test case using SST (contour levels trimmed at $\mu_t/\mu$ = 500).**

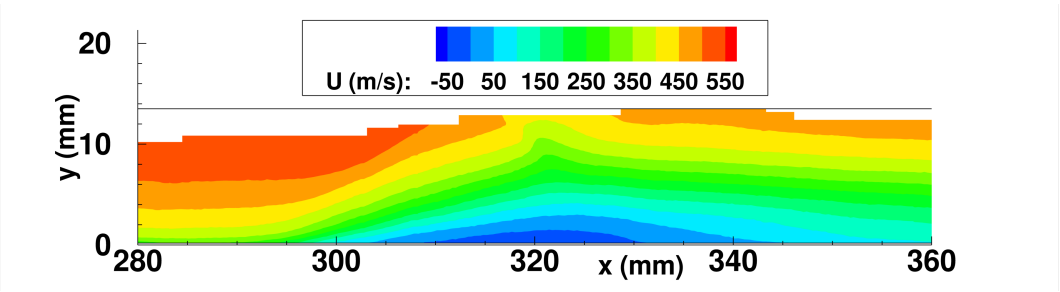


(a) Experiment

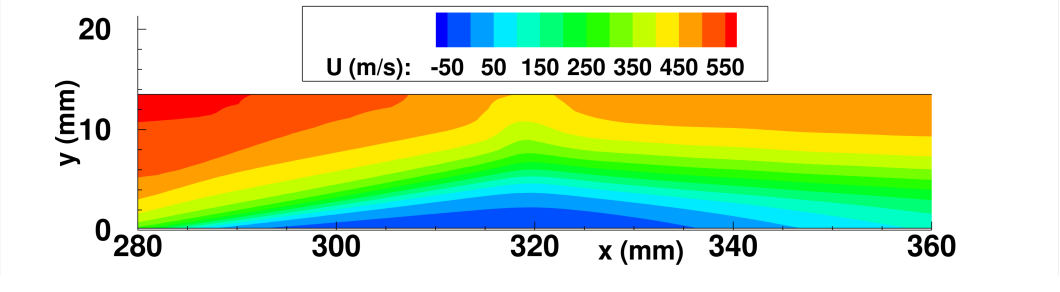


(b) Menter SST

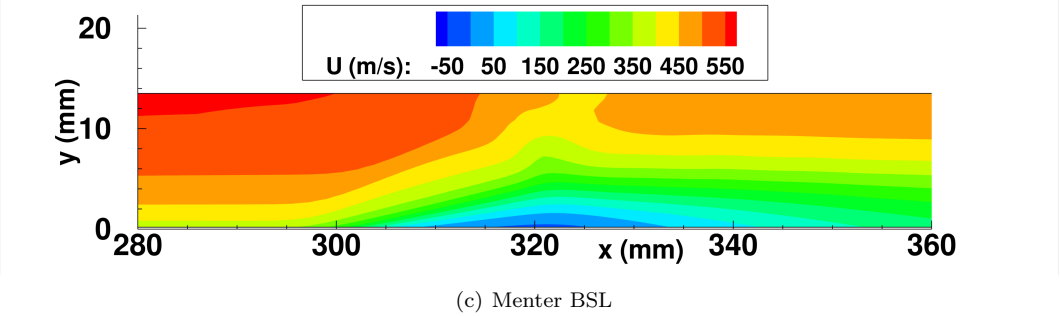


(c) Menter BSL

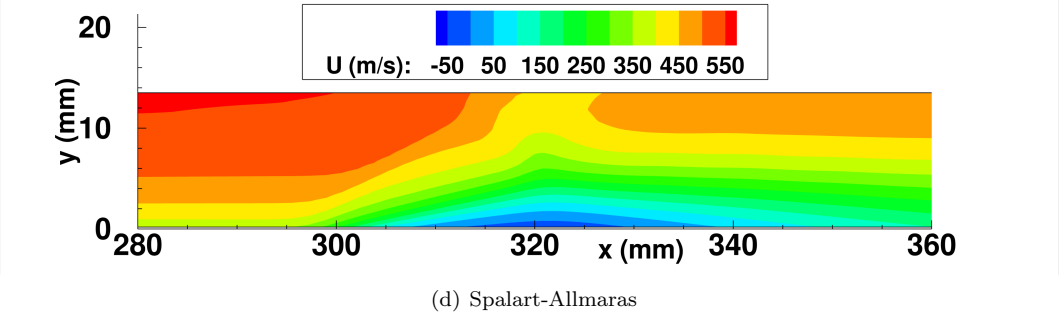


(d) Spalart-Allmaras

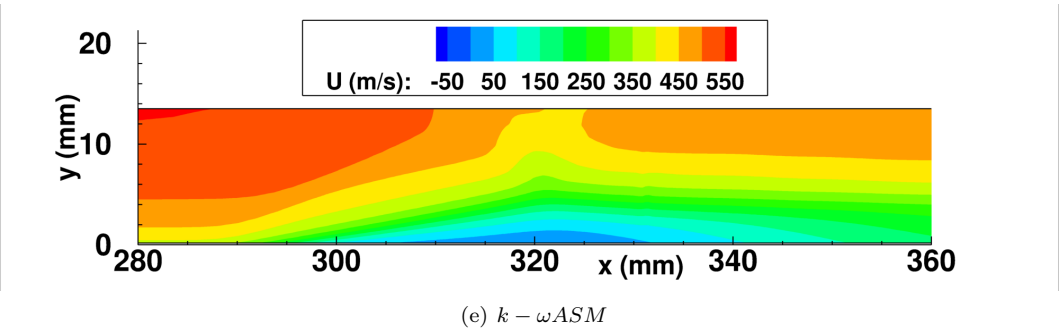


(e) $k-\omega ASM$

**Figure 7. Axial velocity contours for UFAST test case in vicinity of SWTBLI.**

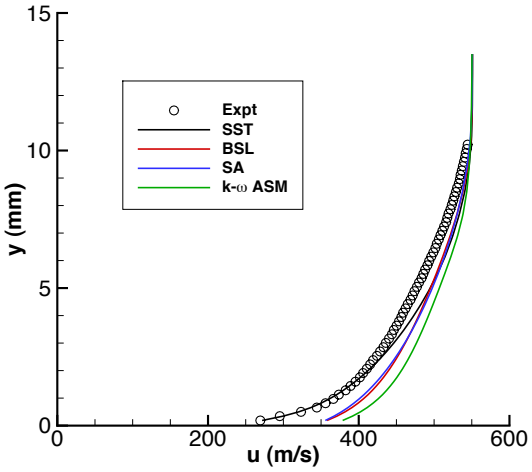


(a) x = 280 mm

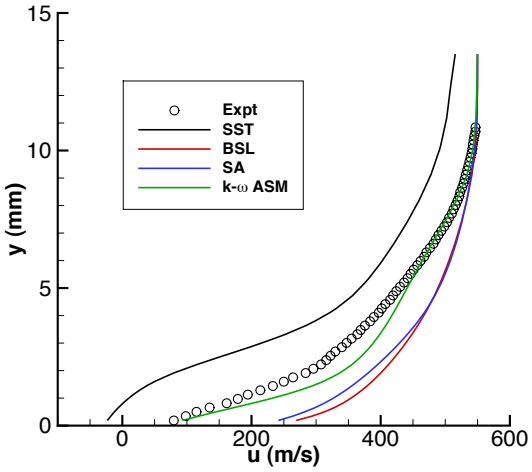


(b) x = 300 mm

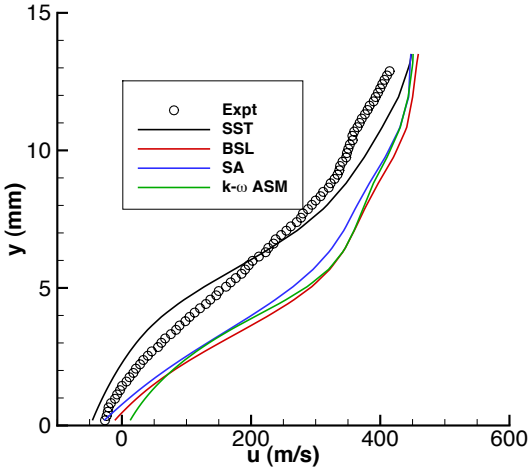


(c) x = 320 mm

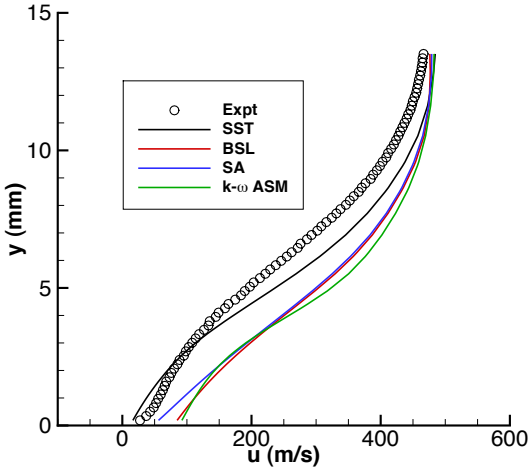


(d) x = 340 mm

**Figure 8. Axial velocity profiles for UFAST test case in vicinity of SWTBLI.**

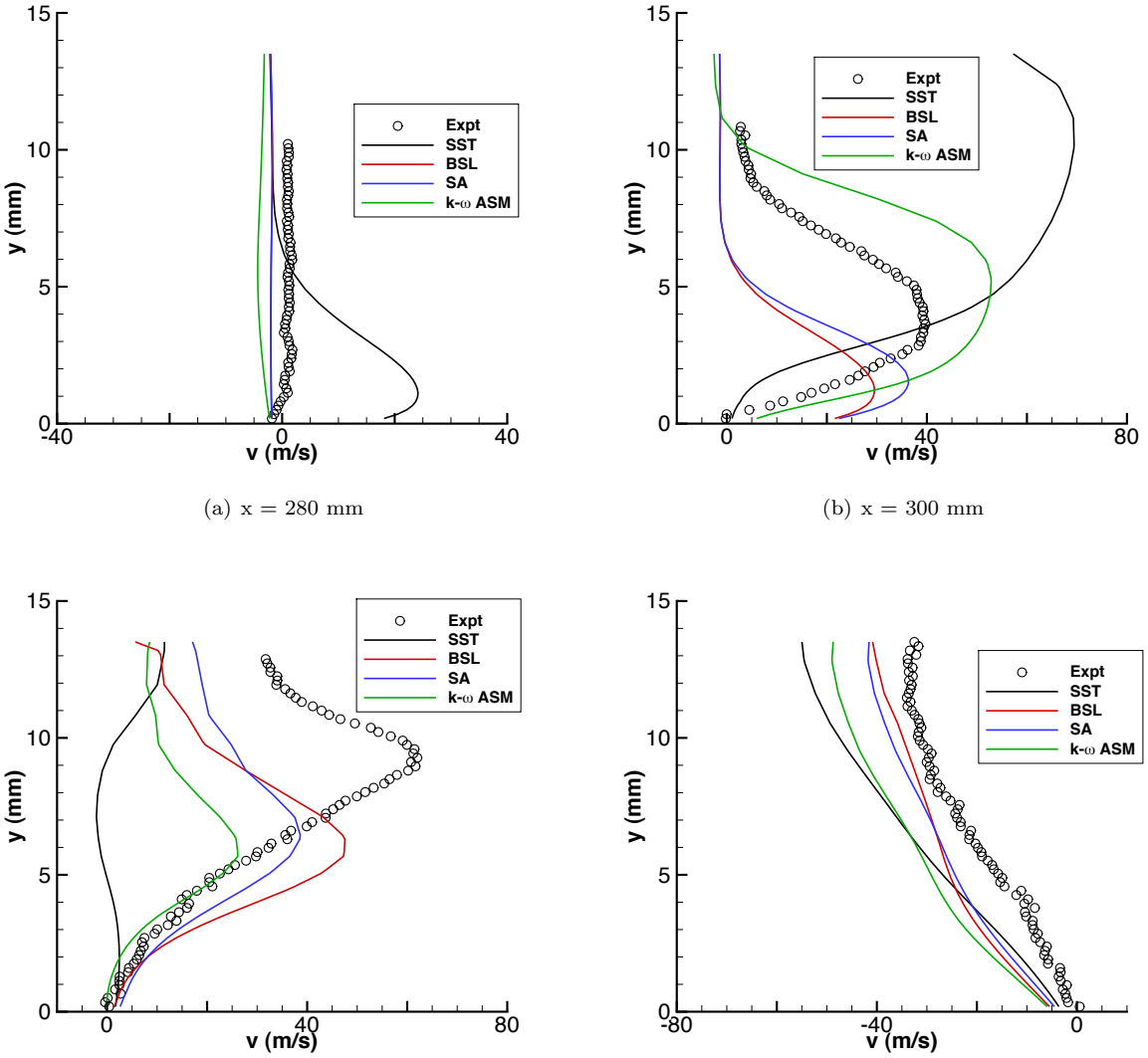


(a) x = 280 mm

(b) x = 300 mm

(c) x = 320 mm

(d) x = 340 mm

**Figure 9. Normal velocity profiles for UFAST test case in vicinity of SWTBLI.**

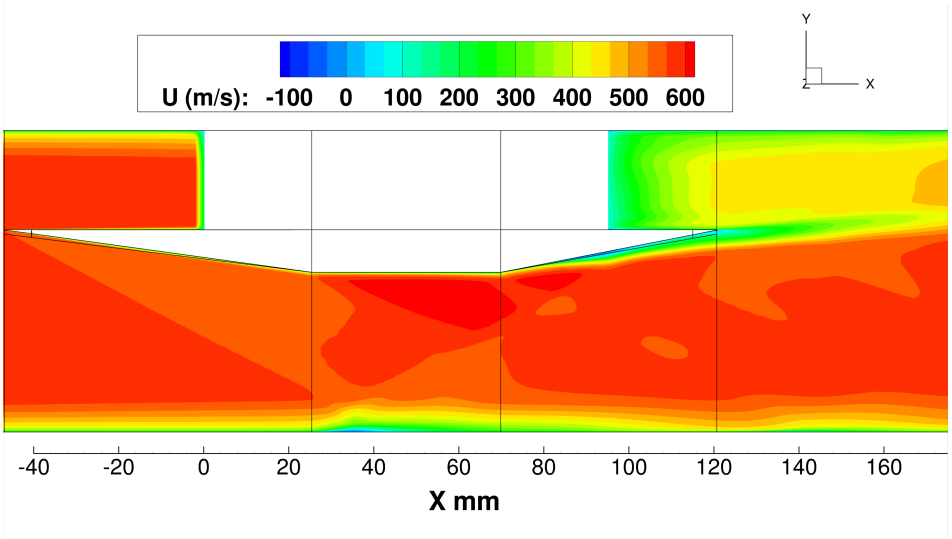


(a) 7.75 degree shock generator

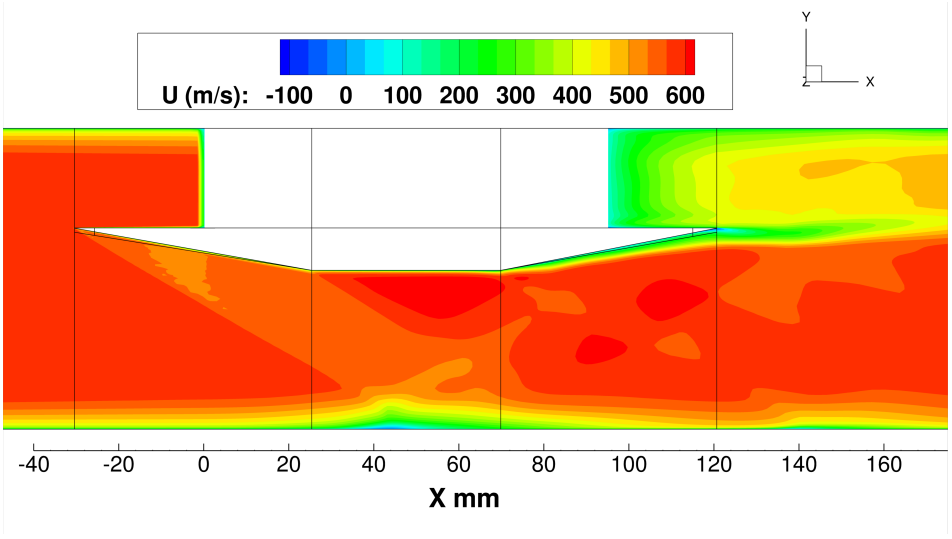


(b) 10 degree shock generator

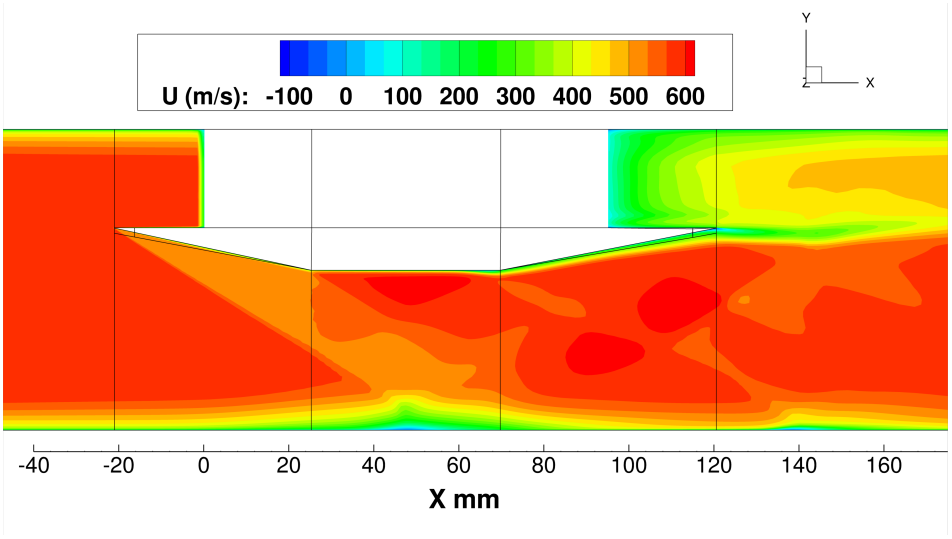


(c) 12 degree degree shock generator

**Figure 10. Axial velocity contours for UM test cases using the SST model.**

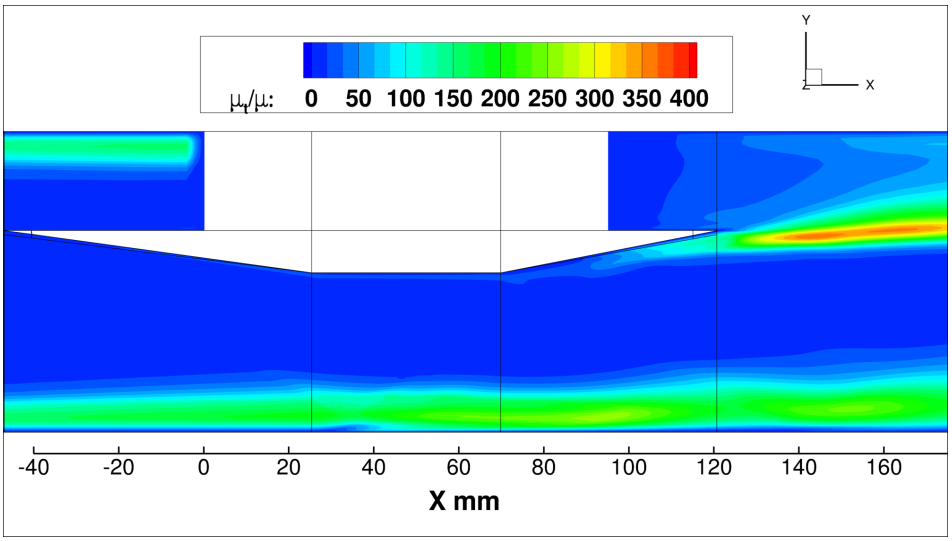


(a) 7.75 degree shock generator

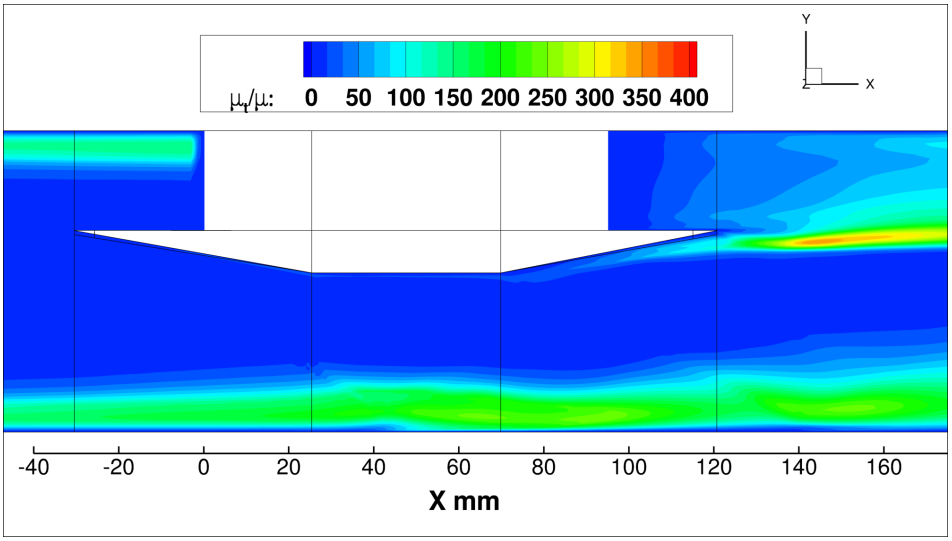


(b) 10 degree shock generator

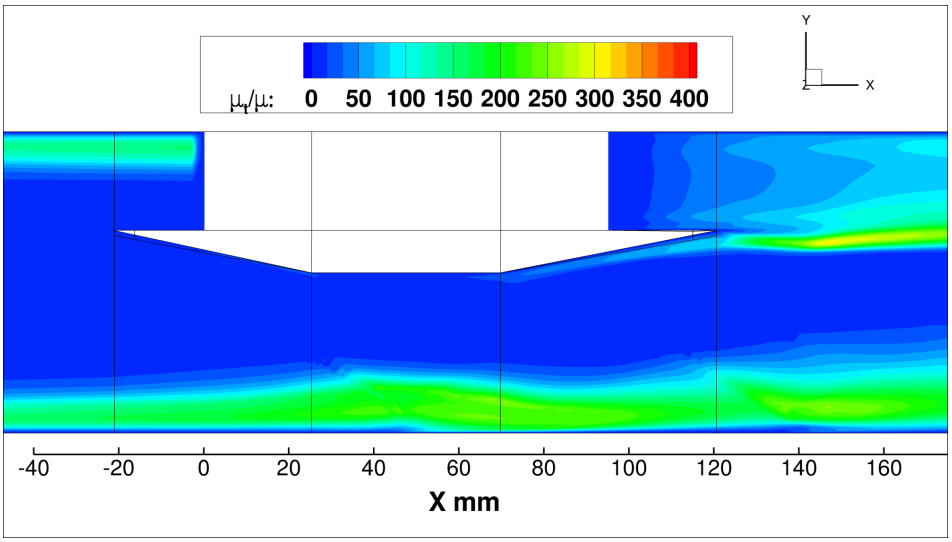


(c) 12 degree degree shock generator

**Figure 11. Eddy viscosity contours for UM test cases using the SST model.**

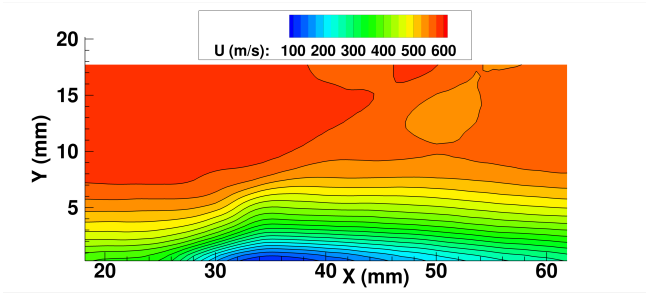


(a) Experiment

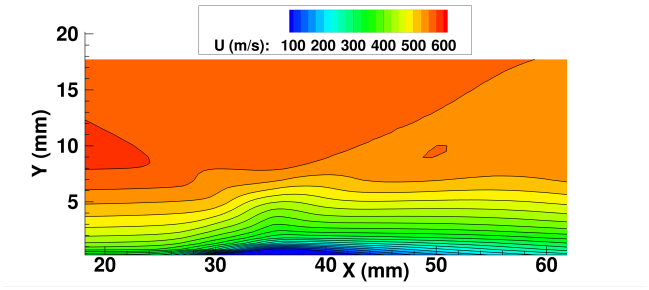


(b) Menter SST

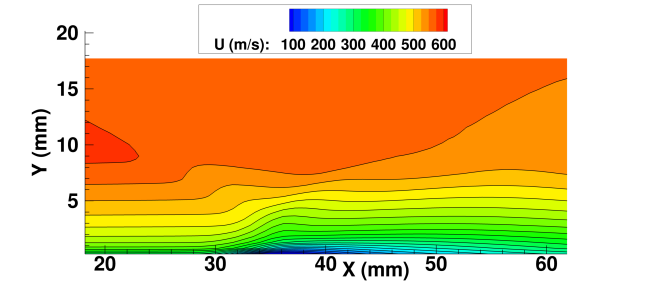


(c) Menter BSL

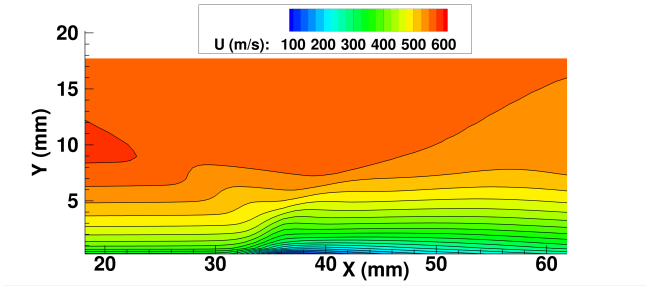


(d) Spalart-Allmaras

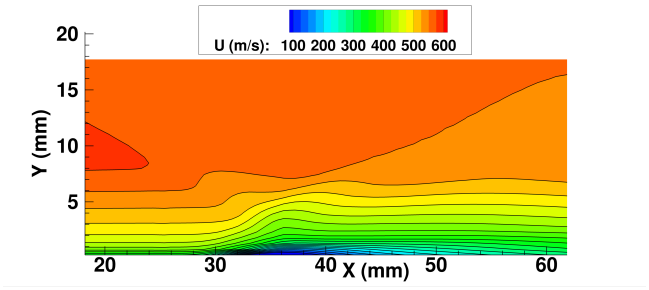


(e) $k-\omega ASM$

**Figure 12. Axial velocity contours for UM test case in vicinity of SWTBLI.**

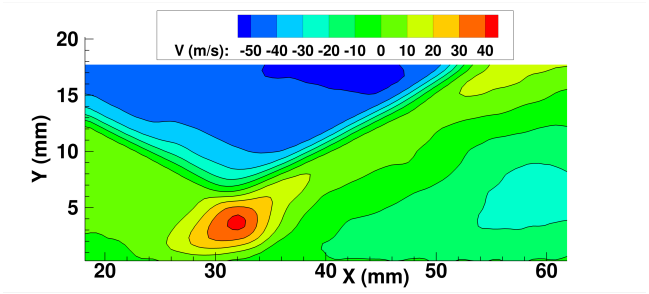


(a) Experiment

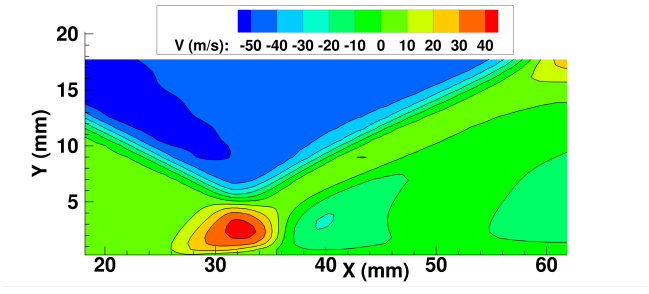


(b) Menter SST

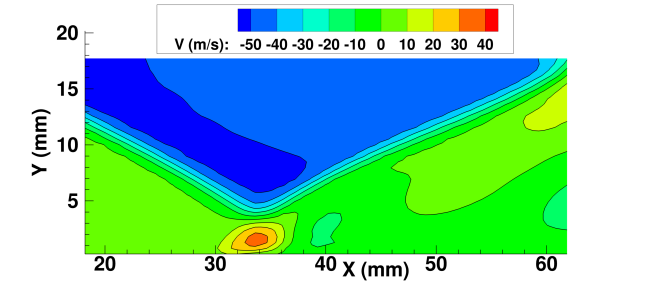


(c) Menter BSL

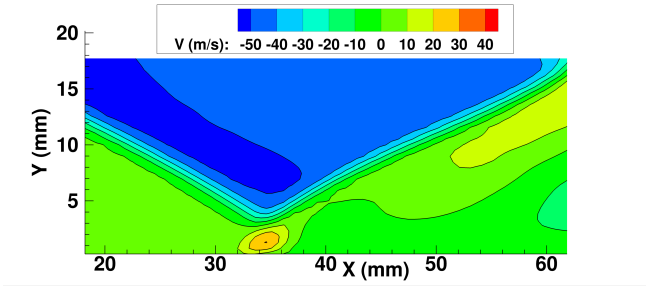


(d) Spalart-Allmaras

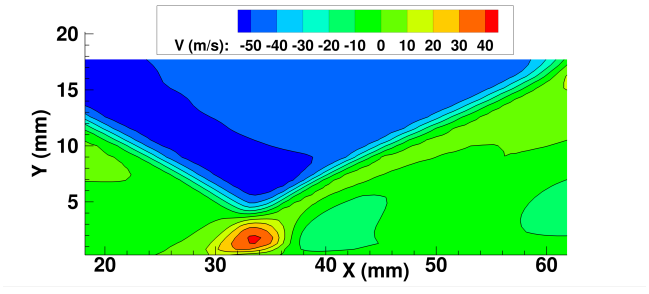


(e) $k-\omega ASM$

**Figure 13. Normal velocity contours for UM test case in vicinity of SWTBLI.**

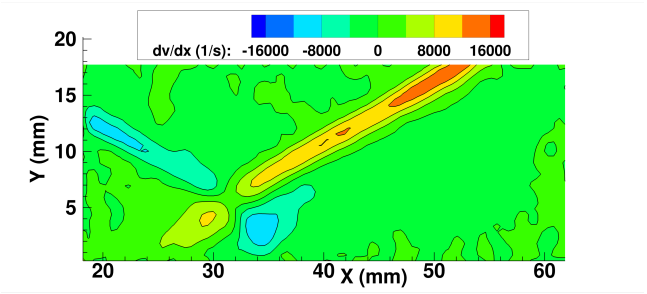


(a) Experiment

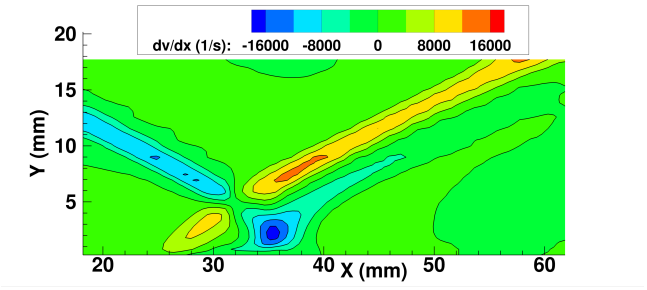


(b) Menter SST

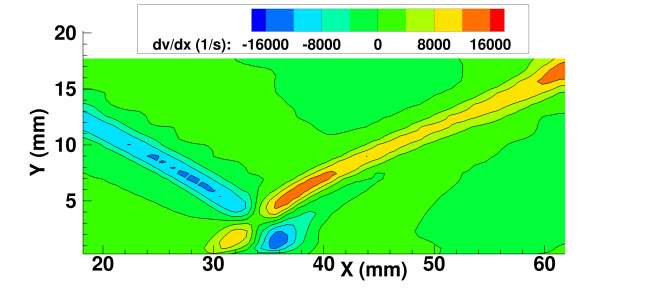


(c) Menter BSL

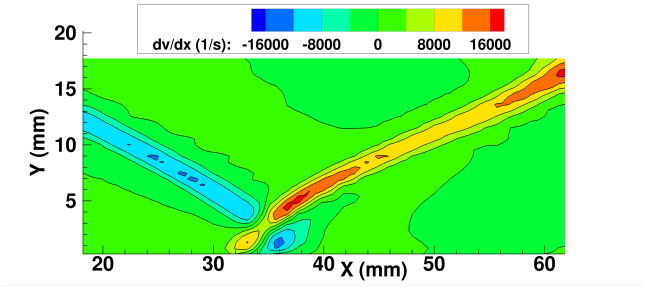


(d) Spalart-Allmaras

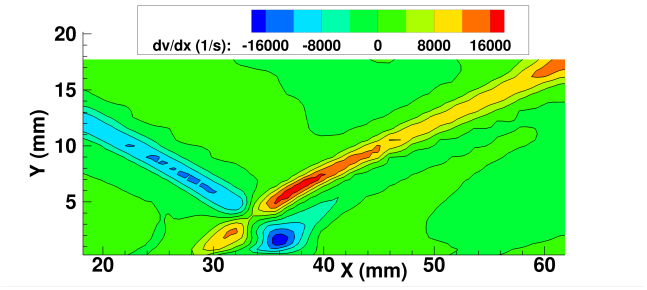


(e) $k-\omega ASM$

**Figure 14.** $dv/dx$ **contours for UM test case in vicinity of SWTBLI.**

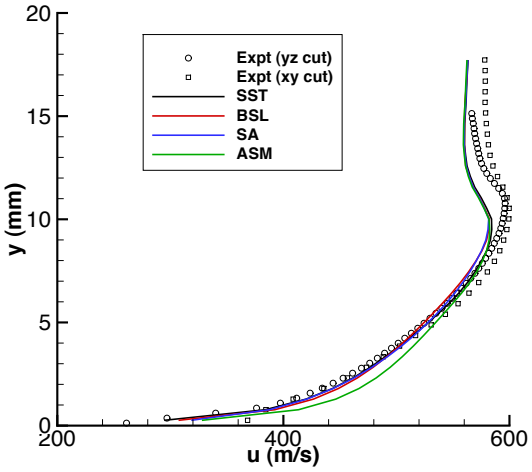


(a) x = 20.76 mm

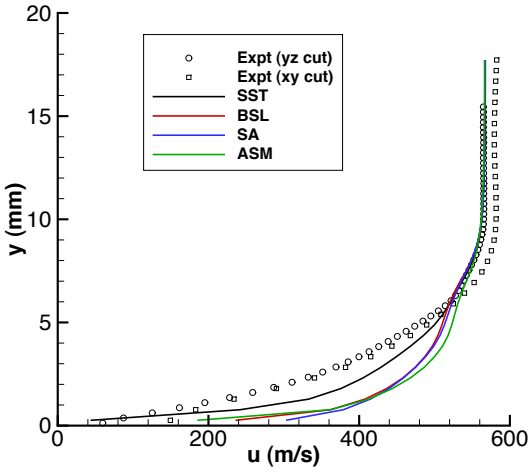


(b) x = 30.76 mm

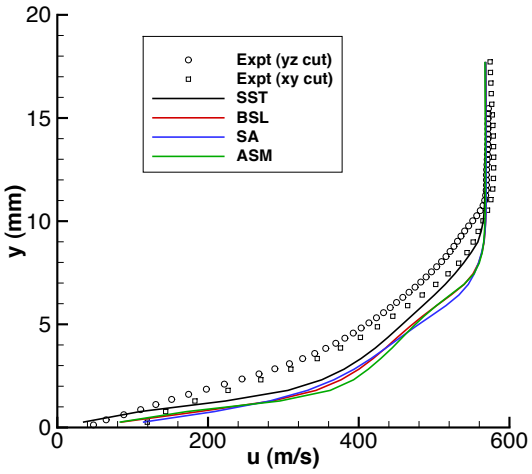


(c) x = 38.76 mm

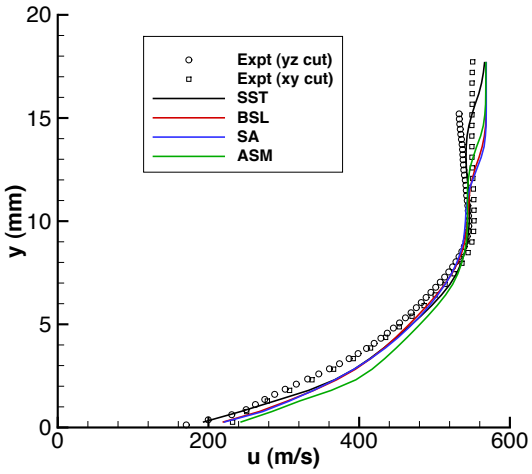


(d) x = 53.76 mm

**Figure 15. Turbulence model effects on axial velocity profiles for UM test case in vicinity of SWTBLI.**

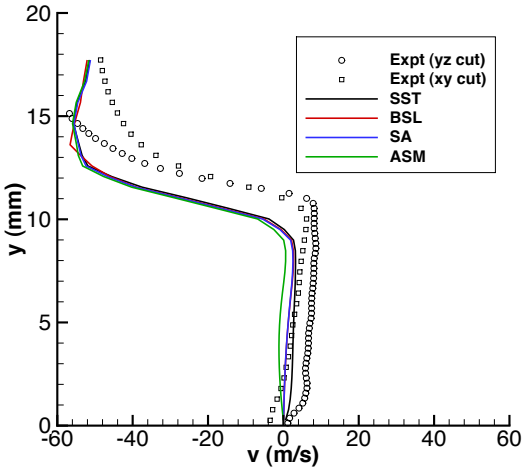


(a) x = 20.76 mm

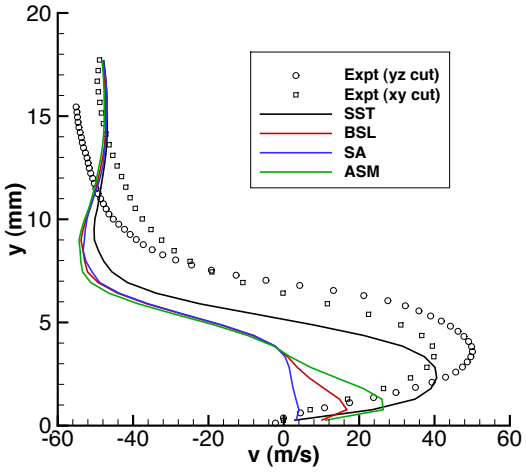


(b) x = 30.76 mm

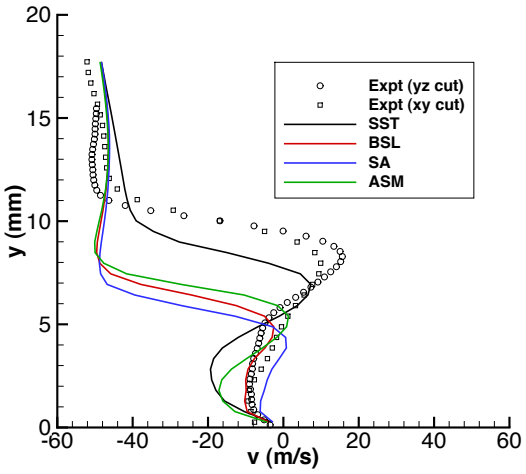


(c) x = 38.76 mm

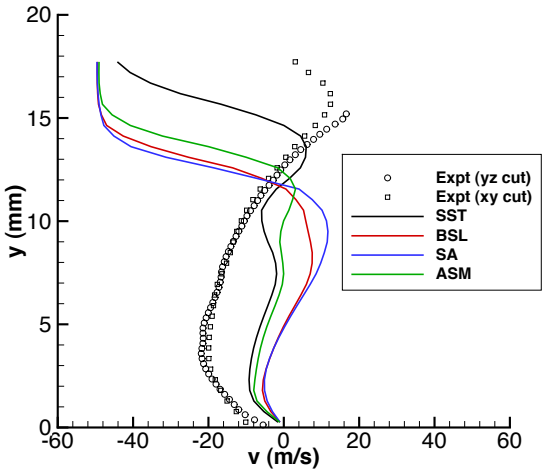


(d) x = 53.76 mm

**Figure 16. Turbulence model effects on normal velocity profiles for UM test case in vicinity of SWTBLI.**

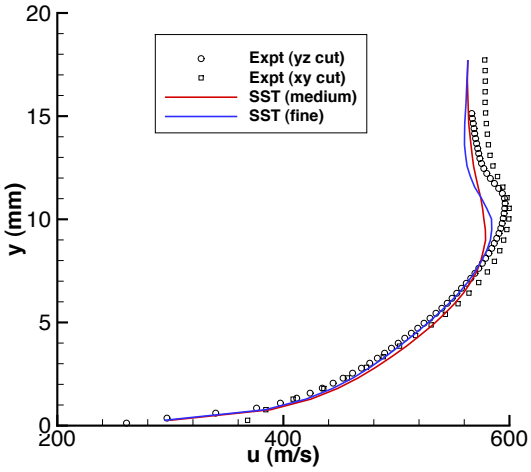


(a) $u$-velocity at x = 20.76 mm

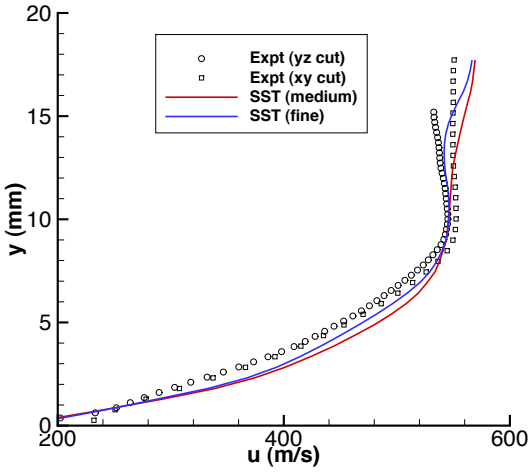


(b) $u$-velocity at x = 53.76 mm

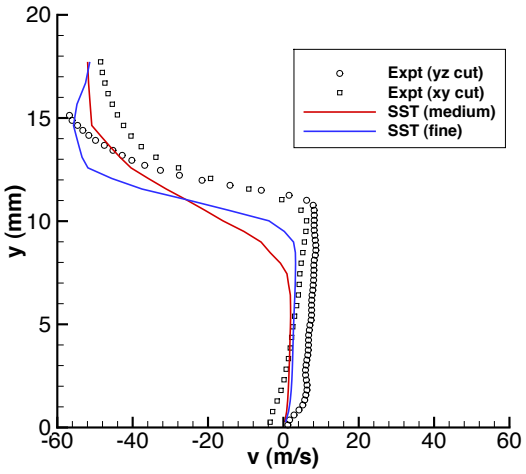


(c) $v$-velocity at x = 20.76 mm

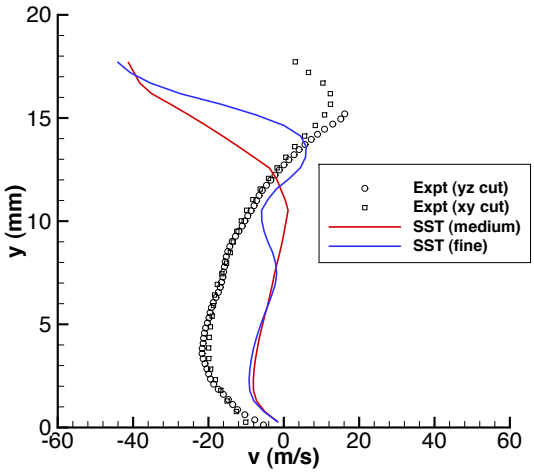


(d) $v$-velocity at x = 53.76 mm

**Figure 17. Effects of grid resolution on velocity profiles for UM test case in vicinity of SWTBLI.**

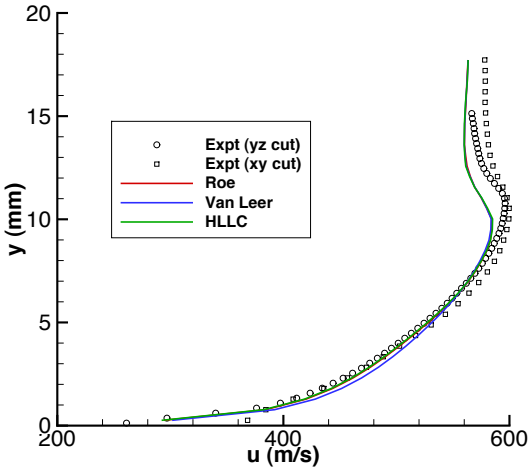


(a) $u$-velocity at x = 20.76 mm

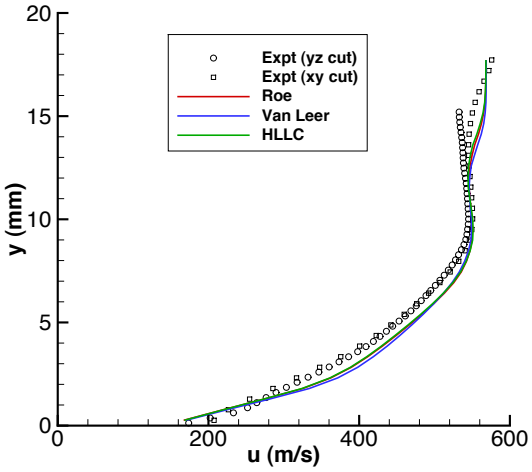


(b) $u$-velocity at x = 53.76 mm

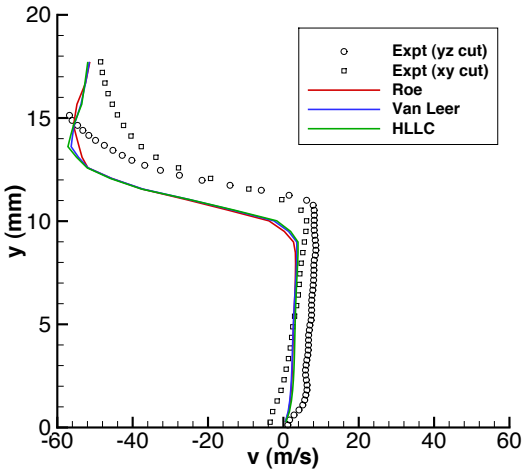


(c) $v$-velocity at x = 20.76 mm

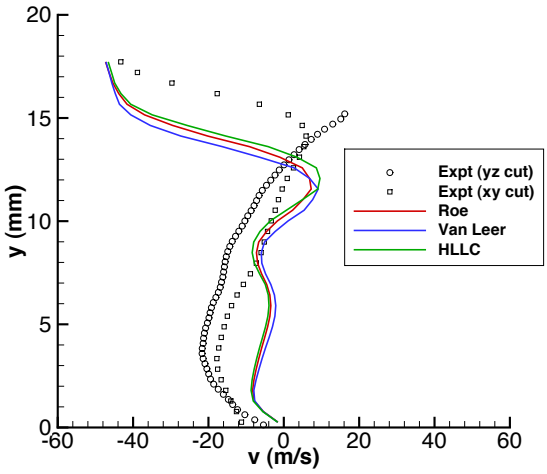


(d) $v$-velocity at x = 53.76 mm

**Figure 18. Effects of upwinding scheme on velocity profiles for UM test case in vicinity of SWTBLI.**

| REPORT DOCUMENTATION PAGE | Form Approved OMB No. 0704-0188 |
|---|---|



| 1. REPORT DATE *(DD-MM-YYYY)* | 2. REPORT TYPE | 3. DATES COVERED *(From - To)* |
|---|---|---|
| 01-02-2013 | Technical Memorandum | |

**4. TITLE AND SUBTITLE**
Wind-US Code Contributions to the First AIAA Shock Boundary Layer Interaction Prediction Workshop

**5a. CONTRACT NUMBER**

**5b. GRANT NUMBER**

**5c. PROGRAM ELEMENT NUMBER**

**6. AUTHOR(S)**
Georgiadis, Nicholas, J.; Vyas, Manan, A.; Yoder, Dennis, A.

**5d. PROJECT NUMBER**

**5e. TASK NUMBER**

**5f. WORK UNIT NUMBER**
WBS 599489.02.07.03.03.13.01

**7. PERFORMING ORGANIZATION NAME(S) AND ADDRESS(ES)**
National Aeronautics and Space Administration
John H. Glenn Research Center at Lewis Field
Cleveland, Ohio 44135-3191

**8. PERFORMING ORGANIZATION REPORT NUMBER**
E-18611

**9. SPONSORING/MONITORING AGENCY NAME(S) AND ADDRESS(ES)**
National Aeronautics and Space Administration
Washington, DC 20546-0001

**10. SPONSORING/MONITOR'S ACRONYM(S)**
NASA

**11. SPONSORING/MONITORING REPORT NUMBER**
NASA/TM-2013-217837

**12. DISTRIBUTION/AVAILABILITY STATEMENT**
Unclassified-Unlimited
Subject Category: 02
Available electronically at http://www.sti.nasa.gov
This publication is available from the NASA Center for AeroSpace Information, 443-757-5802

**13. SUPPLEMENTARY NOTES**

**14. ABSTRACT**
This report discusses the computations of a set of shock wave/turbulent boundary layer interaction (SWTBLI) test cases using the Wind-US code, as part of the 2010 American Institute of Aeronautics and Astronautics (AIAA) shock/ boundary layer interaction workshop. The experiments involve supersonic flows in wind tunnels with a shock generator that directs an oblique shock wave toward the boundary layer along one of the walls of the wind tunnel. The Wind-US calculations utilized structured grid computations performed in Reynolds-averaged Navier-Stokes mode. Four turbulence models were investigated: the Spalart-Allmaras one-equation model, the Menter Baseline and Shear Stress Transport k-ω two-equation models, and an explicit algebraic stress k-ω formulation. Effects of grid resolution and upwinding scheme were also considered. The results from the CFD calculations are compared to particle image velocimetry (PIV) data from the experiments. As expected, turbulence model effects dominated the accuracy of the solutions with upwinding scheme selection indicating minimal effects.

**15. SUBJECT TERMS**
Turbulence; Boundary-layer; Shock-wave; Computational fluid dynamics

| 16. SECURITY CLASSIFICATION OF: | | | 17. LIMITATION OF ABSTRACT | 18. NUMBER OF PAGES | 19a. NAME OF RESPONSIBLE PERSON |
|---|---|---|---|---|---|
| a. REPORT | b. ABSTRACT | c. THIS PAGE | | | STI Help Desk (email:help@sti.nasa.gov) |
| U | U | U | UU | 30 | 19b. TELEPHONE NUMBER *(include area code)* 443-757-5802 |